



## Emissions of CFCs, HCFCs and HFCs from India

Daniel Say<sup>1</sup>, Anita L. Ganesan<sup>2</sup>, Mark F. Lunt<sup>3</sup>, Matthew Rigby<sup>1</sup>, Simon O'Doherty<sup>1</sup>, Chris Harth<sup>4</sup>, Alistair J. Manning<sup>5</sup>, Paul B. Krummel<sup>6</sup>, and Stephane Bauguitte<sup>7</sup>

<sup>1</sup>School of Chemistry, University of Bristol, Bristol, BS8 1TS, UK

<sup>2</sup>School of Geographical Sciences, University of Bristol, Bristol BS8 1SS, UK

<sup>3</sup>School of Geosciences, University of Edinburgh, Edinburgh, EH9 3JW, UK

<sup>4</sup>Scripps Institution of Oceanography, University of California, San Diego, La Jolla, USA

<sup>5</sup>Met Office Hadley Centre, Exeter, EX1 3PB, UK

<sup>6</sup>Climate Science Centre, CSIRO Oceans and Atmosphere, Aspendale, Australia

<sup>7</sup>Facility for Airborne Atmospheric Measurements, Cranfield University, MK43 0AL, UK

**Correspondence:** Daniel Say (Dan.Say@bristol.ac.uk)

**Abstract.** As the second most populous country and third fastest growing economy, India has emerged as a global economic power. As such, its emissions of greenhouse and ozone-depleting gases are of global significance. However, unlike neighbouring China, the Indian sub-continent is very poorly monitored by existing measurement networks. Of the greenhouse/ozone-depleting gases, India's emissions of synthetic halocarbons (here defined as chlorofluorocarbons (CFCs), hydrochlorofluorocarbons (HCFCs) and hydrofluorocarbons (HFCs)) are not well-known. Previous measurements from the region have been obtained at observatories many hundreds of miles from source regions, or at high altitudes, limiting their value for the estimation of regional emission rates. Given the projected rapid growth in demand for refrigerants in India, emission estimates of these halocarbons are urgently needed, to provide a benchmark against which future changes can be evaluated. In this study, we report the first atmospheric-measurement derived emissions of the ozone-depleting CFCs and HCFCs, and potent greenhouse gas HFCs from India. Air samples were collected at low-altitude during a 2-month aircraft campaign between June and July 2016. Emissions were derived from measurements of these samples using an inverse modelling framework and evaluated to assess India's progress in phasing out ozone-depleting substances (ODS) under the Montreal Protocol. Our CFC estimates show that India contributed 52 (26 – 83) Tg CO<sub>2</sub>eq yr<sup>-1</sup>, which were 7 (4 – 12) % of global emissions in 2016. HCFC-22 emissions at 7.8 (6.0 – 9.9) Gg yr<sup>-1</sup> were of similar magnitude to emissions of HFC-134a (8.2 (6.1 – 10.7) Gg yr<sup>-1</sup>), suggesting that India used a range of HCFC and HFC refrigerants in 2016. We estimated India's HFC-23 emissions to be 1.2 (0.9 – 1.5) Gg yr<sup>-1</sup> and our results are consistent with resumed venting of HFC-23 by HCFC-22 manufacturers following the discontinuation of funding for abatement under the Clean Development Mechanism. We report small emissions of HFC-32 and HFC-143a and provide evidence that HFC-32 emissions were primarily due to fugitive emissions during manufacturing processes. Lack of significant correlation among HFC species and the small emissions derived for HFC-32 and HFC-143a indicate that in 2016, India's use of refrigerant blends R-410A, R-404A and R-507A was limited, despite extensive consumption elsewhere in the world.



*Copyright statement.* TEXT

## 1 Introduction

Chlorofluorocarbons (CFCs) were used widely around the world for refrigeration, air-conditioning and foam blowing (Montzka et al., 1999) until they were found to deplete stratospheric ozone (Wallington et al., 1994). These species were thus regulated  
5 under the Montreal Protocol on Substances that Deplete the Ozone Layer. The adoption of the Montreal Protocol and its amendments subsequently led to a marked reduction in emissions of ozone-depleting substances (ODS) (Derwent et al., 1998; Velders et al., 2007). However, emissions are expected to continue, particularly from developing (Article 5) nations (Vollmer et al., 2009; Wan et al., 2009), predominantly from banked sources such as refrigerators and rigid foams (Vollmer et al., 2009). While the emissions of many ODS are declining, broadly in line with expectations, the emissions of some species, CFC-11 in  
10 particular, have not reduced in the last decade, and are now increasing (Montzka et al., 2018). The reason for rising emissions of this gas is not yet known, although evidence suggests new production, likely originating from Asia, which has not been reported to the United Nations Environment Programme (UNEP).

As a consequence of the Montreal Protocol, emissions of the first-generation of CFC replacements, the hydrochlorofluorocarbons (HCFCs), species with similar thermodynamic properties to CFCs but reduced ozone-depletion potentials (ODP),  
15 increased considerably in the 1990s and 2000s (Montzka et al., 2009). Because HCFCs still have non-zero ODPs, they were subsequently also regulated under the Copenhagen Amendment to the Montreal Protocol in 2004. Article 5 countries are currently permitted to emit HCFCs but began their HCFC phase-out in 2013, with reduction targets outlined by the HCFC phase-out management plan (HPMP (UNDP, 2013)). Recently, it was reported that global emissions of the three major HCFCs (HCFC-22, HCFC-141b and HCFC-142b) had stabilised or were decreasing, largely due to decreasing emissions from the  
20 developed world (Montzka et al., 2014; Simmonds et al., 2017).

Following regulation of HCFCs, the second-generation replacements, hydrofluorocarbons (HFCs) were adopted because they do not appreciably deplete stratospheric ozone. However, their high Global Warming Potentials (GWP, Table 1) mean that HFCs contribute to global climate change, leading to recent efforts to reduce consumption. The 2016 Kigali Amendment to the Montreal Protocol set out targets for a gradual phase-down of HFC production and consumption. The first cuts by most Article  
25 5 countries will not be required until 2024 and a small number of these countries will not be required to freeze emissions until 2028. Except for HFC-23 (Simmonds et al., 2018), whose emissions are a by-product of HCFC-22 production, and HFC-152a, whose emissions have stabilised since 2010 (Simmonds et al., 2016), global emissions of all major HFCs were rising until at least the end of 2016 (Simmonds et al., 2017).

India, an Article 5 country under the Montreal Protocol, ratified the Protocol in 1992. A complete phase-out of CFCs was  
30 mandated in India by 2010. Except for use in metered dose inhalers, which ceased in 2010, India reported a complete phase-out of both the production and consumption of CFCs in 2008 (UNDP, 2013). Emissions from existing banks, such as old refrigeration appliances, are however, likely to persist. Following phase-out of CFCs, India was required to reduce emissions of HCFCs. Under Stage I of the HPMP, production and consumption of HCFCs for dispersive use was designated to be frozen



by January 1st, 2016, followed by complete phase-out by 2040. At the 19th Meeting of the Parties in 2007, India agreed to an acceleration of this schedule. Under Stage II of the HPMP, India agreed to freeze its consumption of HCFCs at the base level (2009/10 average) by 2013, followed by a 10% reduction (relative to the base level) by 2015 and a complete phase-out by 2030. In 2016, India adopted the Kigali Amendment, under which it will also begin to phase-down its production and consumption of HFCs. However, its developing status means it will not be required to make its first reductions until 2028, and in the meantime, India's demand for HFCs is expected to rise dramatically (Purohit et al., 2016).

With a population exceeding one billion and a rapidly expanding economy, India's ODS and HFC emissions are expected to have global significance. Based on inferred consumption trends, Velders et al. (2015) estimated that India will emit 400 Tg CO<sub>2</sub>eq yr<sup>-1</sup> of HFCs in 2050, a 67-fold increase over 2016 emissions. However, little else is known about India's emissions. Estimates from bottom-up, inventory-based methods have only been made for a subset of HFCs (HFC-134a, HFC-152a and HFC-23) in India and only up to 2010 (Garg et al., 2006; MoEFCC, 2012, 2015). Emissions of these gases have never been estimated for India through regional 'top-down' or inverse modelling approaches that use atmospheric mole fraction measurements to infer surface fluxes. However, top-down methods have been applied elsewhere in Asia (Palmer et al., 2003; Yokouchi et al., 2005; Kim et al., 2010; Saikawa et al., 2012; Stohl et al., 2010).

Previous studies in other countries have shown that there can be large discrepancies between national inventories of ODS and HFCs and those inferred from atmospheric observations (Graziosi et al., 2017; Lunt et al., 2015; Say et al., 2016). Therefore, this dual quantification approach has been highlighted by many organizations as being beneficial for accurate and transparent greenhouse gas reporting (Leip et al., 2018). In this study, we present the first top-down emissions estimates of CFCs, HCFCs and HFCs and provide a 2016 benchmark, which is critical for being able to evaluate future policy changes surrounding India's ODS and HFC emissions.

## 2 Materials and Methods

### 2.1 Collection and analysis of air samples

Atmospheric samples were collected in evacuated 3 L stainless steel electro-polished flasks aboard the UK's FAAM (Facility for Airborne Atmospheric Measurements) BAe-146 research aircraft. In total 176 samples were collected over 11 flights conducted between the 12th June and 9th July 2016 (Table 2). On nine of these flights, samples were collected over northern India at altitudes ranging predominantly between 0 – 1.5 km (Fig. 1). Air was drawn through a forward-facing air sampling pipe on the exterior of the aircraft and pressurised into the sample flasks using a metal bellows pump (Senior Aerospace PWSC 28823-7). Sample flasks were evacuated to 1x10e<sup>-5</sup> psig prior to each flight. Before sample collection, the lines within each sample case were flushed with ambient air for a minimum of one minute. Sample flasks were filled to a maximum pressure of 41 psig, giving a usable sample volume of 9 L at atmospheric pressure. Sample filling typically varied between 25 - 60 seconds in duration, depending on altitude (equivalent to ~7 km of flight track at average cruise velocity). Canisters were filled at regular intervals during each flight (interval dependent on flight length). When not in use, flask samples were stored in a container with no air-conditioning, to eliminate the risk of sample contamination from leaking air-conditioning refrigerant. None of the



gases discussed here were present on the research aircraft itself, and the laboratory at the University of Bristol does not contain an HFC filled air-conditioning unit. Apart from flasks collected over the Arabian Sea, samples were transported from India to Bristol within 1 month of collection.

Flask samples were analysed using the Medusa GCMS analytical system, with modifications to the analysis routine developed to account for the small volume and low pressure of the flask samples. In the set-up described previously (Miller et al., 2008; Arnold et al., 2012), atmospheric measurements were derived from 2 L samples, injected into the pre-concentration system at a flow rate of  $100 \text{ cm}^3 \text{ min}^{-1}$ , resulting in a total injection time of 20 minutes. For this work, each measurement was derived from three 1.75 L analyses, injected into the analytical system at a flow rate of  $50 \text{ cm}^3 \text{ min}^{-1}$ , resulting in a total injection time of 35 minutes. The analysis of each flask was bracketed by analyses of a quaternary reference gas, to account for short term drifts in detector sensitivity. ODS/HFC mole fractions are reported relative to a set of gravimetrically prepared ‘primary’ standards, maintained at the Scripps Institute of Oceanography (SIO), via a hierarchy of compressed real-air standards held in 34 L electro-polished stainless-steel canisters (Essex Industries, Missouri, USA). The working (quaternary) standard was compared to a tertiary tank on a roughly monthly basis. System blanks were conducted monthly, to quantify possible interferences from system leaks and carrier gas impurities. For each gas, the ratio of target to qualifier ion(s) was continually monitored to ensure that co-eluting species did not interfere with the analyses. For each flask, measurement precision was estimated as the standard deviation of the three replicate analyses. Average measurement precisions are shown in Table 3 and are comparable to the precisions reported previously by Miller et al. (2008).

## 2.2 Numerical Atmospheric Modelling Environment (NAME)

A Lagrangian particle dispersion model was used to quantify the influence of surface fluxes on each atmospheric measurement. The Met Office NAME (Numerical Atmospheric dispersion Modelling Environment) model was run in backwards mode (Manning et al., 2011) to generate 30-day air histories for every minute along each flight path (each minute represents approximately 7 km of the flight track at average speed). These air histories represent the sensitivity of a measurement to fluxes from the surface (defined as 0 - 40 meters above ground level). NAME was driven using meteorological output from the operational analysis of the UK Met Office Numerical Weather Prediction model, the Unified Model, with a horizontal resolution of approximately 17 km in 2016. The model domain spanned from  $55 - 109^\circ \text{E}$  and  $6 - 48^\circ \text{N}$  up to 19 kilometres altitude. For each flight minute, tracer particles were released at a rate of  $1000 \text{ particles min}^{-1}$  from a cuboid, whose dimensions were determined by the change in latitude, longitude and altitude of the aircraft during that one-minute period. In general, samples were collected during level sections of each flight path, minimising transport errors that could arise from the result of releasing particles over a range of altitudes. At the boundaries of the domain, the three-dimensional location and time at which each particle left the domain was recorded to provide the sensitivity to boundary conditions.

The ability of NAME to accurately simulate transport is critical for ensuring robust emission estimates. Model simulated wind direction and speed were compared to meteorological data recorded on board the FAAM aircraft (Fig. S1–S2). To ensure that possible transport errors arising as a result of the inaccurate simulation of meteorological parameters did not affect our posterior estimates, emissions derived using the complete set of atmospheric measurements were compared to those derived from



a filtered dataset (Fig. S3), whereby observations corresponding to periods where the NAME simulated wind speed/direction differed from the measured meteorology by more than 20% were removed.

### 2.3 Inverse modelling using atmospheric dispersion modelling

Our inverse method is based on the trans-dimensional approach described by Lunt et al. (2016). Emissions and uncertainties were characterized using principals of hierarchical Bayesian modelling detailed in Ganesan et al. (2014). The inverse approach solves for a parameter vector,  $\mathbf{x}$  (including flux fields and boundary conditions), using measurement data,  $\mathbf{y}$ . In a Bayesian framework, independent prior knowledge of emissions,  $\mathbf{x}_{ap}$ , is used in conjunction with measurements to solve for a posterior emissions distribution,  $\mathbf{x}$  using a linear model,  $\mathbf{H}$  (Eq. 1).

$$\mathbf{y} = \mathbf{H}\mathbf{x} + \epsilon \quad (1)$$

$\mathbf{H}$  is a Jacobian matrix of sensitivities, here describing the relationship between changes in atmospheric mole fractions and changes in the parameter vector  $\mathbf{x}$ .  $\epsilon$  is uncertainty arising from the model and the measurements. In a traditional Bayesian inversion, uncertainty in  $\mathbf{x}_{ap}$  and the model-measurement uncertainty,  $\epsilon$ , are both assigned prior to the inversion. These uncertainties are often poorly known and rely on a subjective decision by the investigator, but have been shown to significantly impact upon the derived posterior emissions (Peylin et al., 2002; Rayner et al., 1999). To minimize this impact, a hierarchical approach incorporates additional hyper-parameters, which allow for the propagation of ‘uncertainties in these uncertainties’ to the posterior solution.

$$\rho(\mathbf{x}, \theta | \mathbf{y}) \propto \rho(\mathbf{y} | \mathbf{x}, \theta) \cdot \rho(\mathbf{x} | \theta) \cdot \rho(\theta) \quad (2)$$

Eq. 2 is a hierarchical version of Bayes’ theorem (normalizing factor not shown for brevity). In this example, the prior emissions uncertainty is governed by a hyper-parameter ( $\theta$ ), which has a probability density function (PDF) that is explored within the inversion. This equation can also be employed in a similar way for the model-measurement uncertainty or any other unknown parameters. The hierarchical Bayesian approach was extended to a trans-dimensional framework, in which the number and configuration of the spatial grid over which emissions were estimated were also unknown parameters, prior to the inversion. Therefore, it is largely the information content of the measurements that govern these unknown aspects. This framework has been shown to result in a more robust and justifiable quantification of uncertainties in emissions than traditional approaches.

In general, Eq. 2 is not solvable via analytical means and was estimated using Markov Chain Monte Carlo (MCMC). In this application, we used MCMC with a Metropolis-Hastings algorithm. We sampled 320,000 variants of the parameter space with the first 120,000 discarded as ‘burn-in’ to ensure that the system had no knowledge of the initial state. The remaining 200,000 samples were then used to form the posterior PDFs. In our estimates, the means of these posterior PDFs are presented, with the uncertainties represented by the 5<sup>th</sup> and 95<sup>th</sup> percentile values.



Emissions were aggregated into totals for the northern-central India (NCI) region. The majority of gases, whose sources are expected to be distributed by population, were scaled to a national total using the NCI emissions and population statistics. For HFC-23, the NCI region incorporated 4 of the 5 known manufacturing plants for HCFC-22. To estimate national emissions, we scaled the NCI total by the ratio of HCFC-22 produced at those four factories, to total production at all five (based on 5 2015 factory specific production statistics (UNEP, 2017)). Based on these statistics, over 98% of HCFC-22 was produced by factories residing within the NCI. HFC-32 was not scaled to an Indian total, since results show that the distribution for this gas within India is not likely to be population-based.

While the estimates presented here represent emissions over a two-month period, they are likely to be consistent with annual emissions of gases that are not expected to have significant seasonality in India. Seasonality in global emissions of HFC-134a 10 and HCFC-22 has been reported previously (Xiang et al., 2014), but India's tropical/subtropical climate may minimize this variation. In addition, due to sampling by aircraft, our emissions estimates are likely to be representative of a regional-scale for gases that have sources that are widespread and do not vary significantly in time. These characteristics are thought to be true for most gases studied here. For gases with some episodic emissions, which we show to be the case for HFC-125, additional caution must be made in their interpretation.

## 15 2.4 A priori emissions

A priori emissions were assembled from a variety of sources owing to the limited information available for India. **CFCs**: since a total ban on CFC production and consumption has now been in place since 2010, country specific emissions/consumption data no longer exist. Despite this, studies suggest that emissions of these gases are ongoing (Montzka et al., 2018). To estimate a priori total emissions over India, we scaled an estimate of 2016 global emissions derived using the AGAGE 12-box model (an 20 extension of Rigby et al. (2014)) by population statistics (India accounted for approximately 17.7% of the global population and was therefore assumed a priori to account for 17.7% of global CFC emissions). **HCFCs**: a priori total HCFC emissions over India were based on 2015 consumption data reported by India in its HPMP Stage II Road Map report (MoEFCC, 2017). Consumption is expected to be an underestimate of emissions due to the presence of banked sources such as refrigerators and foams. However, a large uncertainty was assigned to the prior. **HFCs**: excluding HFC-23, prior HFC emission totals for India 25 were calculated by dividing the 2010 EDGAR v4.2 (European Commission, 2009) Asian continental total by population (with India accounting for approximately 29% of the Asian total). This was done because EDGAR does not indicate any emissions from India. For HFC-23, prior emission totals for India were based on the 2010 HFC-23 emissions reported in India's Biennial Update Report to the United Nations Framework Convention on Climate Change (MoEFCC, 2015), and extrapolated to 2016 using reported HCFC-22 production data (and assuming a constant co-production ratio) (MoEFCC, 2017).

30 No spatial information was available for any of the ODS/HFCs studied here. For all gases, prior emissions totals were distributed across the model domain using the National Oceanic and Atmospheric Administration (NOAA) DMSP-OLR satellite night light data, available at the increment of 30 arc second ([https://ngdc.noaa.gov/eog/data/web\\_data/v4composites/](https://ngdc.noaa.gov/eog/data/web_data/v4composites/)). The night lights distribution was a useful starting point for our emissions maps, since night lights are generally correlated with populated density (Raupach et al., 2010), but are also likely to include industrial sites, such as HCFC-22 manufacturing plants.



Night-lights reflect where anthropogenic activity is present but does not weight the emissions a priori according to intensity. We expected the major sources of HFCs, HCFCs and CFCs (refrigeration and air-conditioning and insulating foam) to be explicitly linked to domestic and/or commercial activities, or from industries requiring a significant work-force.

In all gases, the prior was assigned a large uncertainty ( $1 \times 10^{-5}$  times the prior), to reflect the very limited current understanding of Indian spatial ODS/HFC emissions and ensure that our flux estimates were informed overwhelmingly by the atmospheric observations. To ensure that the derived results were independent of the prior used, we compared results derived using the night light-based prior with those derived with a uniform distribution (Fig. S3).

## 2.5 A priori boundary conditions

The footprints from NAME consider only emissions released within the model domain. Hence, a prior estimate of the mole fraction at the boundaries of model domain must be made and incorporated into the modelled mole fraction. To this end, mole fraction ‘curtains’ of each gas were used to provide a priori information about boundary conditions (it should be noted that these boundary conditions were adjusted within the inversion). For the HFCs, mole fractions were simulated using the 3D global chemical transport model MOZART (Model for OZone and Related chemical Tracers (Emmons et al., 2010)). MOZART was driven by offline meteorological fields from MERRA (Modern Era Retrospective-Analysis for Research and Applications (Rienecker et al., 2011)). For the HCFCs and CFCs, MOZART fields were not available, and uniform curtains were assumed. The mole fraction for each curtain in each month was estimated using the AGAGE 12-box model (Rigby et al., 2014) and measurements from five baseline AGAGE observatories. For each gas, the model was used to estimate a monthly baseline mole fraction for four latitude bands. The simulated mole fraction from latitude bands  $30 - 90^\circ \text{N}$ ,  $0 - 30^\circ \text{N}$  and  $0 - 30^\circ \text{S}$  were used to assign a priori mole fractions to the North, East and West and South curtains of the model domain respectively. The boundary conditions associated with each NAME-simulated measurement were calculated by mapping the exit times and locations of particles leaving the domain to the curtains. In the inversion, a decomposition of the a priori boundary conditions, represented as offsets to the curtains in the North, East, West and South directions, were solved for in the inversion in addition to emissions.

## 2.6 Global halocarbon emissions estimation

Indian ODS/HFC emissions were compared to global emission estimates calculated using the AGAGE 12-box model (Rigby et al., 2014), assimilating data from five remote AGAGE background sites (Mace Head, Ireland; Trinidad Head, USA; Ragged Point, Barbados; Cape Matatula, American Samoa and Cape Grim, Tasmania) following a Bayesian inversion methodology. Baseline monthly means were estimated by statistically filtering the high-frequency data (O’Doherty et al., 2001). The data were averaged into semi-hemispheres ( $30^\circ \text{N} - 90^\circ \text{N}$ ,  $0^\circ \text{N} - 30^\circ \text{N}$ ,  $30^\circ \text{S} - 0^\circ \text{S}$ ,  $90^\circ \text{S} - 30^\circ \text{S}$ ) for comparison with mole fractions predicted by the AGAGE 12-box model, which resolves these four semi-hemispheres, with vertical levels separated at 500 and 200 hPa (Cunnold et al., 1983; Rigby et al., 2013). The model uses annually repeating meteorology and OH concentrations from Spivakovsky et al. (2000), tuned to match the growth rate of methyl chloroform. Temperature-dependent rate constants from Burkholder et al. (2015) for the reaction of each halocarbon with OH were used, leading to lifetimes in the



model of 51.9, 101.3, 92.7, 11.6, 9.2, 17.6, 13.3, 54.4, 30.7, 1.5, 5.3 and 237.4 years for CFC-11, CFC-12, CFC-113, HCFC-22, HCFC-141b, HCFC-142b, HFC-134a, HFC-143a, HFC-125, HFC-152a, HFC-32 and HFC-23 respectively. A Bayesian framework was used to derive emissions from the data and the model, in which an a priori estimate of the emissions growth rate was adjusted to bring the model into agreement with the data (following Rigby et al. (2011)). The inversion propagates 5 uncertainties in the observations through to the derived fluxes and augments the derived fluxes with uncertainties due to the lifetime and potential errors in the calibration scale. These estimates are a 2016 extension of those presented in Rigby et al. (2014).

### 3 Results

#### 3.1 Atmospheric Measurements

10 Measurements were made from whole air flask samples collected over India during June and July 2016. Fig. 1 shows the location and altitude of these measurements along with the model-derived sensitivity of these samples to surface emissions. The region broadly corresponding to maximum surface sensitivity from our samples is denoted as northern-central India (NCI), where 72% of India's population is found (SEDAC, 2016). Mole fractions of each ODS and HFC measured during the campaign are shown in Fig. 2. For comparison, each gas is shown alongside baselines representative of the Northern and Southern 15 Hemispheres. These baselines were derived from statistical fits to observations from the Advanced Global Atmospheric Gases Experiment (AGAGE) sites at Mace Head, Ireland and Cape Grim, Tasmania (Prinn et al., 2018). Although all of the samples collected during our campaign were within the Northern Hemisphere, the South Asian monsoon, which occurs annually between June and September, draws air from southern latitudes, resulting in the Indian regional background being more consistent with the Southern Hemisphere at this time of year. For CFC-12 and CFC-113, owing to the decrease in emissions resulting from 20 the Montreal Protocol, the hemispheric baselines are now similar and the difference in mole fraction between hemispheres is smaller than the average precision of our flask measurements.

Enhancements in mole fractions over the regional background form the basis for estimating regional emissions. For all species except HFC-134a (Supporting Information), the average mole fractions of samples collected over the Arabian Sea were lower than those collected directly over NCI due to the prevailing westerly winds that bring well-mixed oceanic air to the 25 Indian subcontinent during these months. Back trajectory analysis confirmed that these samples had not interacted with any other significant land mass in the 30 days prior to collection. Variability in the mole fraction of samples collected over NCI varied considerably by species. For CFC-11, CFC-12 and CFC-113, few pollution events were observed, and their signals were of similar size to the measurement precision. Similarly, only small enhancements were observed for HCFC-142b, suggesting its main use as a foam-blowing agent was not significant or was not widespread and thus could not be discerned in the aircraft 30 samples.

In contrast, large enhancements in mole fraction were observed for HFC-134a and HCFC-22, suggesting that usage of these substances as a refrigerant is widespread. It is likely that these gases share a range of common sources, including use in India's largest refrigeration and air-conditioning sector, stationary air-conditioning (Purohit et al., 2016). We find a significant ( $R =$





0.53, Fig. 3) relationship between HFC-134a and HCFC-22 mole fractions, supporting this assertion. Large enhancements in HFC-23 mole fraction suggest that the samples were sensitive to emissions from HCFC-22 manufacturing facilities, as HFC-23 is a by-product of HCFC-22 production. The NCI region contains four out of the five Indian manufacturing facilities that were registered under the Clean Development Mechanism (CDM) (<https://cdm.unfccc.int/Projects/registered.html>).

5 Enhancements were also observed in HFC-32 and HFC-125, although the observed mole fractions for these species were not strongly correlated ( $R = 0.15$ , Fig. 3), suggesting that India is yet to adopt refrigerant blend R-410A (50% by wt. HFC-125, 50% by wt. HFC-32) on a large scale. In a recent study, Kim et al. (2010) reported a similarly weak relationship for measurements representative of Chinese emissions, suggesting that the two largest Asian economies are yet to adopt the commonly used refrigerant blend R-410A. In contrast, HFC-125/HFC-32 measurements at Mace Head over the same time-period were  
10 strongly correlated ( $R = 0.86$ ). All enhancements in HFC-32 are found to correspond with enhancements in another halocarbon, dichloromethane ( $\text{CH}_2\text{Cl}_2$ , Fig. 3), a commonly used solvent that is also used as a feedstock in the production of HFC-32. The significance of this correlation is discussed further in section 3.2.3.

We found no correlation for HFC-125 and HFC-143a ( $R = -0.04$ , Fig. 3), gases whose emissions are regularly linked through the consumption of blends R-404A (52% by wt. HFC-143a, 44% by wt. HFC-125, 4% by wt. HFC-134a) and R-507A (50%  
15 by wt. HFC-125, 50% by wt. HFC-143a) (Montzka et al., 2014; O'Doherty et al., 2014). In contrast, at Mace Head, a strong HFC-125/HFC-143a correlation ( $R = 0.78$ ) was observed during this time.

Evidence for widespread use of both HCFCs and HFCs and the lack of large enhancements in CFCs suggests that India's transition to first- and second-generation CFC replacements is nearing completion. However, there appears to be little evidence for the consumption of HFC blends or HFC-152a in 2016, refrigerants/propellant used extensively in the developed world  
20 (Greally et al., 2007; O'Doherty et al., 2014).

During two flights (B959 and B963) conducted on the 21<sup>st</sup> and 25<sup>th</sup> of June, a small number of samples were collected over the Arabian Sea. NAME back-trajectory analysis was used to show that these samples had not interacted with any significant landmass in the 30 days prior to collection. Except for HFC-134a, the measurements derived from these samples exhibited very little variation, and the mole fractions were amongst the lowest observed during the campaign, which was consistent with the  
25 oceanic trajectories. As such, these provided a useful constraint upon the baseline for the modelling studies. In contrast, four of the six samples collected on these flights exhibited an elevated HFC-134a concentration, which did not correlate with any other species, including HCFC-22. Several possible explanations exist for these elevated measurements: 1) Flasks collected over the Arabian Sea were compromised due to long storage times (over 1 month) at temperatures exceeding 40 °C before transport back to the UK for analysis. Long-term tests on the stability of HFC-134a at these temperatures have not been conducted; 2)  
30 the enhancements were the result of ship-borne emissions from the Indian Ocean. These flights were at low-altitude (0.01 – 0.8 km) and could have resulted in the measurement of sporadic emissions from ship-based air conditioning systems.



### 3.2 ODS and HFC emissions estimates for NCI and India

Mean NCI and Indian emissions estimates and the relative contributions of each gas to 2016 global emissions are shown in Fig. 4 and tabulated in Table 4 ( $\text{Gg yr}^{-1}$ ) and Table 5 ( $\text{Tg CO}_2\text{eq yr}^{-1}$ ). Uncertainties presented throughout correspond to the 5<sup>th</sup> and 95<sup>th</sup> percentiles of the posterior distribution.

5 We estimate 2016 CFC, HCFC and HFC emissions to be 52 (26 – 83)  $\text{Tg CO}_2\text{eq yr}^{-1}$ , 15 (11 – 19)  $\text{Tg CO}_2\text{eq yr}^{-1}$  and 50 (38 – 64)  $\text{Tg CO}_2\text{eq yr}^{-1}$  respectively, which correspond to 7 (4 – 12) %, 2 (1 – 3) % and 6 (5 – 8) % of global emissions. There are no previous top-down national-scale estimates of any of these gases for India. In 2016, India's HFC emissions were approximately an order of magnitude larger than the 2016 emissions assumed by Velders et al. (2015), suggesting that future projections of India's HFC emissions could be inaccurate.

#### 10 3.2.1 CFCs

Through commitments under the Montreal Protocol, India finalised its phase-out of the consumption and production of CFCs in 2010. However, residual emissions from banks (refrigerators, foams, landfills etc.) are expected to continue for several decades (Rigby et al., 2014). Our mean CFC-11, CFC-12 and CFC-113 emissions are 1.7 (0.8 – 3.1)  $\text{Gg yr}^{-1}$ , 4.1 (2.1 – 6.3)  $\text{Gg yr}^{-1}$  and 0.5 (0.2 – 0.8)  $\text{Gg yr}^{-1}$ , respectively, corresponding to 2 (1 – 4) %, 13 (7 – 20) %, and 7 (2 – 11) % of global emissions in  
15 2016. For all CFCs studied here, these percentages are smaller than India's percentage population of the global total (17.7% in 2016 (SEDAC, 2016)). The magnitude of the uncertainties in our CFC estimates are largely a reflection of the precision of the measurements. Further work is needed through additional high-precision measurements, particularly for CFC-12, to narrow this uncertainty. For CFC-11, our 2016 estimate of 1.2 (0.6 – 2.2)  $\text{Gg yr}^{-1}$  suggests that NCI, the region with the majority of  
20  $\text{yr}^{-1}$ ) reported between 2013 – 2016 (Montzka et al., 2018).

#### 3.2.2 HCFCs

There is limited information about HCFC emissions from India, with the current state of knowledge encapsulated only in reports of production and consumption (MoEFCC, 2017). We find that India's 2016 HCFC emissions are dominated by HCFC-22 at 7.8 (6.0 – 9.9)  $\text{Gg yr}^{-1}$ , and these emissions comprise only 2 (1 – 3) % of global emissions. Our HCFC-22 emissions  
25 are comparable in magnitude to HFC-134a and HFC-125, discussed below, suggesting that India's transition from HCFCs to their non-ozone depleting replacements is in progress. India's HCFC-22 emissions are considerably smaller than those from other nations such as China, whose emissions in 2007 were estimated at 165 (140 – 213)  $\text{Gg yr}^{-1}$  (Vollmer et al., 2009) and the USA, whose emissions in 2014 were estimated at 40.0 (34.1 – 45.8)  $\text{Gg yr}^{-1}$  (Hu et al., 2017).

Our estimates of India's HCFC-141b and HCFC-142b emissions are small (1.0 (0.7 – 1.5)  $\text{Gg yr}^{-1}$  and 0.10 (0.06 – 0.14)  
30  $\text{Gg yr}^{-1}$ , respectively). Taken together with the small reported consumption of these gases in 2015, our results suggest that either these substances have not had widespread usage in India or that efforts have been made by India under Stage I of the HPMP to phase-out HCFC consumption in the foam sector (MoEFCC, 2017), in favour of zero-ODP alternatives (UNDP,



2013). However, without detailed emissions information from previous years, it is not possible to determine whether the latter has been in effect.

### 3.2.3 HFCs

India's HFC emissions are dominated by emissions of HFC-134a and HFC-125, with estimated rates of 8.2 (6.1 – 10.7) Gg yr<sup>-1</sup> and 6.4 (5.2 – 7.8) Gg yr<sup>-1</sup> respectively. These emissions correspond to 4 (3 - 5) % and 10 (8 - 12) % of global emissions. There are significant discrepancies between previous bottom-up estimates and our top-down results. Garg et al. (2006) estimated Indian HFC-134a emissions to be 1.1 Gg yr<sup>-1</sup> in 2005, while India reported 0 Gg yr<sup>-1</sup> in 2010 in its Biennial Update Report to the United Nations Framework Convention on Climate Change (UNFCCC) (MoEFCC, 2015). While there are no top-down comparisons for 2005, our results show there could have been significant growth in emissions of HFC-134a since 2005 and/or large discrepancies between bottom-up and top-down methodologies.

Further work and additional measurements are required to better understand the non-refrigerant blend sources of HFC-125. Our results suggest a possible application of HFC-125 in India as a standalone refrigerant, or an application that is not currently for HCFC-22 replacement. Possible contributors are fire suppression, use as a solvent and the production of HFC-125 for export. While our model was able to capture most of the signals for the gases studied here (Fig. 5), it was unable to simulate some of the elevated measurements for HFC-125, indicating that in addition to widespread, constant sources, there could be point sources of HFC-125 that are episodic and difficult to resolve in a model.

We estimate India's emissions of HFC-143a to be 0.8 (0.4 – 1.2) Gg yr<sup>-1</sup>, which comprise 3 (1 - 4) % of global emissions. Our low HFC-143a estimate corroborates our assertion of minimal R-404A and R-507A consumption. There are no previous estimates for Indian HFC-143a emissions.

India's HFC-152a emissions are estimated to be 1.2 (0.9 – 1.4) Gg yr<sup>-1</sup>, which amount to 2 (2 - 3) % of global emissions. Garg et al. (2006) estimated India's HFC-152a emissions to be 0.04 Gg yr<sup>-1</sup> in 2005 and attributed these to the glass industry. Our emission rate is comparatively large, suggesting that either there are discrepancies with inventory methodologies or that there has been substantial growth in emissions in the last decade. Regardless, these emissions are small compared to other countries, particularly China, whose emissions of HFC-152a were estimated at 16 Gg yr<sup>-1</sup> in 2013 (Fang et al., 2016), and the USA, for which an emission rate of 51.5 (35.5 – 75.5) Gg yr<sup>-1</sup> was estimated for 2012 (Simmonds et al., 2015).

HFC-32 emissions are estimated for NCI to be 0.44 (0.36 – 0.54) Gg yr<sup>-1</sup>. All the measured enhancements in HFC-32 are correlated with enhancements in dichloromethane, a feedstock in the manufacture of HFC-32 (Fig. 3). These measurements suggest that India's HFC-32 emissions originate predominantly from fugitive losses during the manufacturing process, rather than widespread use in a refrigerant blend. Our assertion is consistent with a previous study (Leedham Elvidge et al., 2015), which attributed growth in South Asian emissions of DCM to HFC-32 manufacture. Since our NCI HFC-32 estimate is attributed to production, we consider it to be decoupled from population density, and hence we have not scaled this value to a national total.



HFC-23 emissions are estimated for India to be 1.2 (0.9 – 1.5) Gg yr<sup>-1</sup>, which comprise 10 (7 - 12) % of global emissions. Fig. 6 shows that emission ‘hot-spots’ picked out by the inverse model are consistent with the known locations of HCFC-22 manufacturing facilities.

### 3.3 India’s HFC-23 emissions and the Clean Development Mechanism

5 Between 2004 and 2013, India received substantial funding from the Clean Development Mechanism for the abatement of HFC-23 produced during the manufacture of HCFC-22. To assess the impact of the CDM on India’s HFC-23 emissions, we compare our HFC-23 emission estimate to previous estimates derived from bottom-up methods (Fig. 7). Emissions between 1990 and 2005 are from Garg et al. (2006), and in 2007 and 2010 are from India’s reports to the UNFCCC (MoEFCC, 2012, 2015). The reported bottom-up estimates show accelerating growth in India’s HFC-23 emissions, which increased from 0.07  
10 Gg yr<sup>-1</sup> in 1990 to 1.43 Gg yr<sup>-1</sup> in 2010. It is important to note that there is a large discrepancy in emissions reported in the UNFCCC inventory and in the manufacturers’ CDM submissions, suggesting inconsistencies in the two methodologies. These discrepancies highlight the value of independent top-down estimates.

Depending on the efficiency of the manufacturing process, the HFC-23/HCFC-22 production ratio can vary between 0.014 (Rotherham, 2004) for optimised processes to values in excess of 0.04 for inefficient processes (McCulloch and Lindley,  
15 2007). The production ratio is equal to the quantity of HFC-23 produced with respect to the quantity of HCFC-22 produced and is equivalent to an HFC-23 emission ratio when no abatement technologies are implemented. Based on India’s HCFC-22 production statistics and bottom-up HFC-23 emission estimates, in 2007, prior to when all five manufacturers of HCFC-22 reported the use of abatement technologies, the average production ratio was 0.031.

The Clean Development Mechanism was in operation in India between 2004 and 2013. During the period of the CDM when  
20 abatement was in use at all facilities (2009 - 2013, <https://cdm.unfccc.int/Projects/registered.html>), the average emission ratio dropped to 0 – 0.009 based on the amount of non-abated HFC-23 (i.e. emissions vented to the atmosphere) reported by the manufacturing facilities. Our top-down estimate in 2016 corresponds to an average emission ratio of 0.022. While the CDM may have been effective in reducing HFC-23 emissions, our results are consistent with resumed venting of HFC-23 by some or all manufacturers, following the discontinuation of CDM funding. In October 2016, the Indian government issued a national  
25 order requiring all manufacturers of HCFC-22 to maintain a proven abatement system and ensure capacity for the storage of HFC-23 for abatement system down-time. With such systems in place, future growth in India’s HFC-23 emissions may become de-coupled from any growth in HCFC-22 production.

### 3.4 Sensitivity tests

We assessed the sensitivity of derived emissions to the a priori emissions field. For all gases, the two solutions derived using  
30 the spatially-varying and uniform priors were the same within uncertainties, showing our posterior estimates to be robust to the prior used (Fig S3). We also compared the effect of inaccurate transport modelling on derived emissions by using a second, filtered dataset, removing times where NAME wind direction and wind speed differed by more than 20% from the measured parameters. A comparison of original and ‘filtered’ posterior estimates is given in Fig. S3. For all 12 halocarbons, the filtered



estimates were within the uncertainty of the original values, indicating that our estimates were robust with respect to small model transport errors.

#### 4 Conclusions

We present the first national-scale top-down emissions estimates of ODS and HFCs for India. We show that for all of the gases studied here, India's 2016 emissions reflect an emissions profile typical of Article 5 countries, with low emissions of CFCs and large emissions of both HCFCs and HFCs. India's emissions of these gases generally comprise a smaller percentage of global emissions than its 17.7% of the world's population in 2016 would imply. India reported a complete phase-out of CFCs in 2010, however banks such as dated refrigeration equipment, insulating foams and landfill may persist. Our results indicate that India's remaining major CFC emissions represent 7 (4-12) % of global emissions. Of the gases studied here, India's largest emissions are from HFC-134a, HFC-125 and HCFC-22. HFC-134a and HCFC-22 have similar magnitudes of emissions, suggesting that India is in transition between employing HCFC and HFC refrigerants. We present evidence to suggest that India is yet to adopt several common refrigerant blends, including R-410A, R-404A and R-507A, all of which are used extensively in the developed world. India's apparent lack of uptake of refrigerant blends presents as an opportunity for future climate mitigation strategies; if India can be encouraged to bypass HFCs in favour of low-GWP alternatives, substantial CO<sub>2</sub>eq emissions could be avoided. We also show that following discontinuation of funding from the CDM, some or all of India's manufacturers of HCFC-22 likely resumed venting of the HFC-23 by-product. As India's economy expands, projections suggest that its consumption of HFCs will grow significantly. It is important to implement long-term and continuous HFC, HCFC and CFC monitoring from this region of the world to help India evaluate its progress under the Montreal Protocol. Our 2016 estimates provide a benchmark, against which future changes to India's ODS and HFC emissions can be assessed.

#### 5 Code availability

Hierarchical Bayesian trans-dimensional MCMC code is available on request from Anita Ganesan ([Anita.Ganesan@bristol.ac.uk](mailto:Anita.Ganesan@bristol.ac.uk)).

*Author contributions.* D.S. collected the samples, conducted the instrumental analyses, ran the inverse model and wrote the paper. A.G. coordinated the flight campaign, co-developed the inverse model code and aided in the writing of the paper. M.L. co-developed the inverse modelling code and conducted the MOZART model runs. M.R. aided the inverse modelling work. S. O'D. co-conducted the instrumental analyses and provided data from Mace Head. C.H. produced the SIO calibration scales for these gases. A.M. advised on NAME modelling. P.K. provided measurements from Cape Grim. S.B. co-collected the whole air samples.

*Competing interests.* The authors declare that they have no conflict of interest.



*Acknowledgements.* We thank FAAM, Directflight and Avalon Aero personnel for their support during the flight campaign, and the site operators at the Mace Head and Cape Grim stations. We also acknowledge the contribution of the Ministry of Earth Sciences, Government of India, the UK National Environmental Research Council (NERC) and the Monsoon program's UK and Indian principal investigators. Daniel Say was funded by a NERC studentship. Anita Ganesan was supported by a NERC Independent Research Fellowship NE/L010992/1. Mark Lunt was supported by NERC grants NE/I027282/1 and NE/M014851/1. Funding for the field campaign was made possible by NERC grant NE/I027282/1.



## References

- Arnold, T., Mühle, J., Salameh, P. K., Harth, C. M., Ivy, D. J., and Weiss, R. F.: Automated measurement of nitrogen trifluoride in ambient air, *Anal Chem*, 84, 4798–4804, 2012.
- Burkholder, J., Sander, S. P., Abbatt, J., Barker, J. R., Huie, R. E., Kolb, C. E., Kurylo, M. J., Orkin, V. L., Wilmouth, D. M., and Wine, P. H.:  
5 Chemical Kinetics and Photochemical Data for Use in Atmospheric Studies–Evaluation Number 18, NASA panel for data evaluation technical report, 2015.
- Cunnold, D. M., Prinn, R. G., Rasmussen, R. A., Simmonds, P. G., Alyea, F. N., Cardelino, C. A., Crawford, A. J., Fraser, P. J., and Rosen, R. D.: The atmospheric lifetime experiment: 3. Lifetime methodology and application to three years of CFC13 data, *J Geophys Res: Oceans*, 88, 8379–8400, 1983.
- 10 Derwent, R. G., Simmonds, P. G., O’Doherty, S., and Ryall, D. B.: The impact of the Montreal Protocol on halocarbon concentrations in Northern Hemisphere baseline and European air masses at Mace Head, Ireland over a ten year period from 1987–1996, *Atmos Environ*, 32, 3689–3702, 1998.
- Emmons, L. K., Walters, S., Hess, P. G., Lamarque, J., Pfister, G. G., Fillmore, D., Granier, C., Guenther, A., Kinnison, D., and Laepple, T.: Description and evaluation of the Model for Ozone and Related chemical Tracers, version 4 (MOZART-4), *Geosci Model Dev*, 2010.
- 15 European Commission, Joint Research Centre, N. E. A. A. P.: Emission Database for Global Atmospheric Research (EDGAR), release version 4.0, [edgar.jrc.ec.europa.eu](http://edgar.jrc.ec.europa.eu), 2009.
- Fang, X., Velders, G. J. M., Ravishankara, A. R., Molina, M. J., Hu, J., and Prinn, R. G.: Hydrofluorocarbon (HFC) emissions in China: an inventory for 2005–2013 and projections to 2050, *Environ Sci Technol*, 50, 2027–2034, 2016.
- Ganesan, A. L., Rigby, M., Zammit-Mangion, A., Manning, A. J., Prinn, R. G., Fraser, P. J., Harth, C. M., Kim, K.-R., Krummel, P. B., and  
20 Li, S.: Characterization of uncertainties in atmospheric trace gas inversions using hierarchical Bayesian methods, *Atmos Chem Phys*, 14, 3855–3864, 2014.
- Garg, A., Shukla, P. R., , and Kapshe, M.: The sectoral trends of multigas emissions inventory of India, *Atmos Environ*, 40, 4608–4620, 2006.
- Graziosi, F., Arduini, J., Furlani, F., Giostra, U., Cristofanelli, P., Fang, X., Hermanssen, O., Lunder, C., Maenhout, G., and O’Doherty, S.:  
25 European emissions of the powerful greenhouse gases hydrofluorocarbons inferred from atmospheric measurements and their comparison with annual national reports to UNFCCC, *Atmos Environ*, 158, 85–97, 2017.
- Greally, B. R., Manning, A. J., Reimann, S., McCulloch, A., Huang, J., Dunse, B. L., Simmonds, P. G., Prinn, R. G., Fraser, P. J., and Cunnold, D. M.: Observations of 1, 1-difluoroethane (HFC-152a) at AGAGE and SOGE monitoring stations in 1994–2004 and derived global and regional emission estimates, *J Geophys Res: Atmos*, 112, 2007.
- 30 Hu, L., Montzka, S. A., Lehman, S. J., Godwin, D. S., Miller, B. R., Andrews, A. E., Thoning, K., Miller, J. B., Sweeney, C., and Siso, C.: Considerable contribution of the Montreal Protocol to declining greenhouse gas emissions from the United States, *Geophys Res Lett*, 44, 8075–8083, 2017.
- Kim, J., Li, S., Kim, K., Stohl, A., Mühle, J., Kim, S., Park, M., Kang, D., Lee, G., and Harth, C. M.: Regional atmospheric emissions determined from measurements at Jeju Island, Korea: Halogenated compounds from China, *Geophys Res Lett*, 37, 2010.
- 35 Leedham Elvidge, E. C., Oram, D. E., Laube, J. C., Baker, A. K., Montzka, S. A., Humphrey, S., O’Sullivan, D. A., and Brenninkmeijer, C. A. M.: Increasing concentrations of dichloromethane, CH<sub>2</sub>Cl<sub>2</sub>, inferred from CARIBIC air samples collected 1998–2012, *Atmos Chem Phys*, 15, 1939–1958, 2015.



- Leip, A., Skiba, U., Vermeulen, A., and Thompson, R. L.: A complete rethink is needed on how greenhouse gas emissions are quantified for national reporting, *Atmos Environ*, 174, 237–240, 2018.
- Lunt, M. F., Rigby, M., Ganesan, A. L., Manning, A. J., Prinn, R. G., O’Doherty, S., Mühle, J., Harth, C. M., Salameh, P. K., and Arnold, T.: Reconciling reported and unreported HFC emissions with atmospheric observations, *Proc Natl Acad Sci USA*, 112, 5927–5931, 2015.
- 5 Lunt, M. F., Rigby, M., Ganesan, A. L., and Manning, A. J.: Estimation of trace gas fluxes with objectively determined basis functions using reversible-jump Markov chain Monte Carlo, *Geosci Model Dev*, 9, 3213–3229, 2016.
- Manning, A. J., O’Doherty, S., Jones, A. R., Simmonds, P. G., and Derwent, R. G.: Estimating UK methane and nitrous oxide emissions from 1990 to 2007 using an inversion modeling approach, *J Geophys Res: Atmos*, 116, 2011.
- McCulloch, A. and Lindley, A. A.: Global emissions of HFC-23 estimated to year 2015, *Atmos Environ*, 41, 1560–1566, 2007.
- 10 Miller, B. R., Weiss, R. F., Salameh, P. K., Tanhua, T., Grealley, B. R., Mühle, J., and Simmonds, P. G.: Medusa: A sample preconcentration and GC/MS detector system for in situ measurements of atmospheric trace halocarbons, hydrocarbons, and sulfur compounds, *Anal Chem*, 80, 1536–1545, 2008.
- MoEFCC: Second National Communication to the United Nations Framework Convention on Climate Change, 2012.
- MoEFCC: First Biennial Update Report to the United Nations Framework Convention on Climate Change, 2015.
- 15 MoEFCC: HCFC Phase-out Management Plan Stage-II, 2017.
- Montzka, S. A., Butler, J. H., Elkins, J. W., Thompson, T. M., Clarke, A. D., and Lock, L. T.: Present and future trends in the atmospheric burden of ozone-depleting halogens, *Nature*, 398, 690, 1999.
- Montzka, S. A., Hall, B. D., and Elkins, J. W.: Accelerated increases observed for hydrochlorofluorocarbons since 2004 in the global atmosphere, *Geophys Res Lett*, 36, 2009.
- 20 Montzka, S. A., McFarland, M., Andersen, S. O., Miller, B. R., Fahey, D. W., Hall, B. D., Hu, L., Siso, C., and Elkins, J. W.: Recent trends in global emissions of hydrochlorofluorocarbons and hydrofluorocarbons: Reflecting on the 2007 adjustments to the Montreal Protocol, *J Phys Chem A*, 119, 4439–4449, 2014.
- Montzka, S. A., Dutton, G. S., Yu, P., Ray, E., Portmann, R. W., Daniel, J. S., Kuijpers, L., Hall, B. D., Mondeel, D., Siso, C., Nance, J. D., Rigby, M., Manning, A. J., Hu, L., Moore, F., Miller, B. R., and Elkins, J. W.: An unexpected and persistent increase in global emissions
- 25 of ozone-depleting CFC-11, *Nature*, 557, 413, 2018.
- Myhre, G., Shindell, D., Breon, F. M., Collins, W., Fuglestad, J., Huang, J., and Zhang, H.: Anthropogenic and natural radiative forcing Climate Change 2013: The Physical Science Basis. Contribution of Working Group I to the Fifth Assessment Report 576 of the Intergovernmental Panel on Climate Change, *Clim Change*, 423, 658–740, 2013.
- O’Doherty, S., Simmonds, P. G., Cunnold, D. M., Wang, H. J., Sturrock, G. A., Fraser, P. J., Ryall, D., Derwent, R. G., Weiss, R. F., and
- 30 Salameh, P.: In situ chloroform measurements at Advanced Global Atmospheric Gases Experiment atmospheric research stations from 1994 to 1998, *J Geophys Res: Atmos*, 106, 20 429–20 444, 2001.
- O’Doherty, S., Rigby, M., Mühle, J., Ivy, D. J., Miller, B. R., Young, D., Simmonds, P. G., Reimann, S., Vollmer, M. K., and Krummel, P. B.: Global emissions of HFC-143a (CH<sub>3</sub>CF<sub>3</sub>) and HFC-32 (CH<sub>2</sub>F<sub>2</sub>) from in situ and air archive atmospheric observations, *Atmos Chem Phys*, 14, 9249–9258, 2014.
- 35 Organisation, W. M.: Scientific Assessment of Ozone Depletion. Chapter 5: Scenarios, Information, and Options for Policymakers, Tech. rep., 2014.
- Palmer, P. I., Jacob, D. J., Mickley, L. J., Blake, D. R., Sachse, G. W., Fuelberg, H. E., and Kiley, C. M.: Eastern Asian emissions of anthropogenic halocarbons deduced from aircraft concentration data, *J Geophys Res: Atmos*, 108, 2003.





- Peylin, P., Baker, D., Sarmiento, J., Ciais, P., and Bousquet, P.: Influence of transport uncertainty on annual mean and seasonal inversions of atmospheric CO<sub>2</sub> data, *J Geophys Res: Atmos*, 107, 2002.
- Prinn, R. G., Weiss, R. F., Arduini, J., Arnold, T., DeWitt, H. L., Fraser, P. J., Ganesan, A. L., Gasore, J., Harth, C. M., and Hermansen, O.: History of chemically and radiatively important atmospheric gases from the Advanced Global Atmospheric Gases Experiment (AGAGE), *Earth Syst Sci Data*, 10, 985, 2018.
- 5 Purohit, P., Höglund Isaksson, L., Bertok, I., Chaturvedi, V., and Sharma, M.: Scenario Analysis for HFC Emissions in India: Mitigation potential and costs, 2016.
- Raupach, M. R., Rayner, P. J., and Paget, M.: Regional variations in spatial structure of nightlights, population density and fossil-fuel CO<sub>2</sub> emissions, *Energy Policy*, 38, 4756–4764, 2010.
- 10 Rayner, P. J., Enting, I. G., Francey, R. J., and Langenfelds, R.: Reconstructing the recent carbon cycle from atmospheric CO<sub>2</sub>, δ<sup>13</sup>C and O<sub>2</sub>/N<sub>2</sub> observations, *Tellus B*, 51, 213–232, 1999.
- Rienecker, M. M., Suarez, M. J., Gelaro, R., Todling, R., Bacmeister, J., Liu, E., Bosilovich, M. G., Schubert, S. D., Takacs, L., and Kim, G.-K.: MERRA: NASA's modern-era retrospective analysis for research and applications, *J Clim*, 24, 3624–3648, 2011.
- Rigby, M., Manning, A. J., and Prinn, R. G.: Inversion of long-lived trace gas emissions using combined Eulerian and Lagrangian chemical transport models, *Atmos Chem Phys*, 11, 9887–9898, 2011.
- 15 Rigby, M., Prinn, R. G., O'Doherty, S., Montzka, S. A., McCulloch, A., Harth, C. M., Mühle, J., Salameh, P. K., Weiss, R. F., and Young, D.: Re-evaluation of the lifetimes of the major CFCs and CH<sub>3</sub>CCl<sub>3</sub> using atmospheric trends, *Atmos Chem Phys*, 13, 2691–2702, 2013.
- Rigby, M., Prinn, R. G., O'Doherty, S., Miller, B. R., Ivy, D., Mühle, J., Harth, C. M., Salameh, P. K., Arnold, T., and Weiss, R. F.: Recent and future trends in synthetic greenhouse gas radiative forcing, *Geophys Res Lett*, 41, 2623–2630, 2014.
- 20 Rotherham, D.: Greenhouse Gas Emission Reduction Verification Audit for Dupont's Louisville Works Freon-22 Plant, Final Report, ICF Consulting, Toronto, Canada, available online at: [http://cdm.unfccc.int/public\\_inputs/inputam0001/Letter\\_Dupont\\_Annex2\\_03June04.pdf](http://cdm.unfccc.int/public_inputs/inputam0001/Letter_Dupont_Annex2_03June04.pdf), 2004.
- Saikawa, E., Rigby, M., Prinn, R. G., Montzka, S. A., Miller, B. R., Kuijpers, L. J. M., Fraser, P. J. B., Vollmer, M. K., Saito, T., and Yokouchi, Y.: Global and regional emission estimates for HCFC-22, *Atmos Chem Phys*, 12, 10 033–10 050, 2012.
- 25 Say, D., Manning, A. J., O'Doherty, S., Rigby, M., Young, D., and Grant, A.: Re-Evaluation of the UK's HFC-134a Emissions Inventory Based on Atmospheric Observations, *Environ Sci Technol*, 50, 11 129–11 136, 2016.
- SEDAC: Gridded Population of the World, Version 4 (GPWv4): Population Density, 2016.
- Simmonds, P. G., Derwent, R. G., Manning, A. J., McCulloch, A., and O'Doherty, S.: USA emissions estimates of CH<sub>3</sub>CHF<sub>2</sub>, CH<sub>2</sub>FCF<sub>3</sub>, CH<sub>3</sub>CF<sub>3</sub> and CH<sub>2</sub>F<sub>2</sub> based on in situ observations at Mace Head, *Atmos Environ*, 104, 27–38, 2015.
- 30 Simmonds, P. G., Rigby, M., McCulloch, A., Vollmer, M. K., Henne, S., Mühle, J., O'Doherty, S., Manning, A. J., Krummel, P. B., and Fraser, P. J.: Global and regional emissions estimates of 1, 1-difluoroethane (HFC-152a, CH<sub>3</sub>CHF<sub>2</sub>) from in situ and air archive observations, *Atmos Chem Phys*, 16, 365–382, 2016.
- Simmonds, P. G., Rigby, M., McCulloch, A., O'Doherty, S., Young, D., Mühle, J., Krummel, P. B., Steele, P., Fraser, P. J., and Manning, A. J.: Changing trends and emissions of hydrochlorofluorocarbons (HCFCs) and their hydrofluorocarbon (HFCs) replacements, *Atmos Chem Phys*, 17, 4641–4655, 2017.
- 35 Simmonds, P. G., Rigby, M., McCulloch, A., Vollmer, M. K., Henne, S., Mühle, J., O'Doherty, S., Manning, A. J., Krummel, P. B., and Fraser, P. J.: Recent increases in the atmospheric growth rate and emissions of HFC-23 (CHF<sub>3</sub>) and the link to HCFC-22 (CHClF<sub>2</sub>) production, *Atmos Chem Phys*, 18, 4153–4169, 2018.



- Spivakovsky, C. M., Logan, J. A., Montzka, S. A., Balkanski, Y. J., Foreman-Fowler, M., Jones, D. B. A., Horowitz, L. W., Fusco, A. C., Brenninkmeijer, C. A. M., and Prather, M. J.: Three-dimensional climatological distribution of tropospheric OH: Update and evaluation, *J Geophys Res: Atmos*, 105, 8931–8980, 2000.
- Stohl, A., Kim, J., Li, S., O’Doherty, S., Mühle, J., Salameh, P. K., Saito, T., Vollmer, M. K., Wan, D., and Weiss, R. F.: Hydrochlorofluoro-  
5 carbon and hydrofluorocarbon emissions in East Asia determined by inverse modeling, *Atmos Chem Phys*, 10, 3545–3560, 2010.
- UNDP: HCFC Phase-Out Management Plan (HPMP Stage I) for compliance with the 2013 and 2015 control targets for consumption of Annex C Group I substances, <http://www.ozonecell.com/viewsection.jsp?lang=0&id=0,166,400>, 2013.
- UNEP: Key aspects related to HFC-23 by-product control technologies (Decision 78/5), 2017.
- Velders, G. J. M., Andersen, S. O., Daniel, J. S., Fahey, D. W., and McFarland, M.: The importance of the Montreal Protocol in protecting  
10 climate, *Proc Natl Acad Sci USA*, 104, 4814–4819, 2007.
- Velders, G. J. M., Fahey, D. W., Daniel, J. S., Andersen, S. O., and McFarland, M.: Future atmospheric abundances and climate forcings from scenarios of global and regional hydrofluorocarbon (HFC) emissions, *Atmos Environ*, 123, 200–209, 2015.
- Vollmer, M. K., Zhou, L. X., Grealley, B. R., Henne, S., Yao, B., Reimann, S., Stordal, F., Cunnold, D. M., Zhang, X. C., and Maione, M.: Emissions of ozone-depleting halocarbons from China, *Geophys Res Lett*, 36, 2009.
- 15 Wallington, T. J., Schneider, W. F., Worsnop, D. R., Nielsen, O. J., Sehested, J., Debruyn, W. J., and Shorter, J. A.: The environmental impact of CFC replacements HFCs and HCFCs, *Environ Sci Technol*, 28, 320A–326A, 1994.
- Wan, D., Xu, J., Zhang, J., Tong, X., and Hu, J.: Historical and projected emissions of major halocarbons in China, *Atmos Environ*, 43, 5822–5829, 2009.
- Xiang, B., Patra, P. K., Montzka, S. A., Miller, S. M., Elkins, J. W., Moore, F. L., Atlas, E. L., Miller, B. R., Weiss, R. F., and Prinn,  
20 R. G.: Global emissions of refrigerants HCFC-22 and HFC-134a: Unforeseen seasonal contributions, *Proc Natl Acad Sci USA*, 111, 17 379–17 384, 2014.
- Yokouchi, Y., Inagaki, T., Yazawa, K., Tamaru, T., Enomoto, T., and Izumi, K.: Estimates of ratios of anthropogenic halocarbon emissions from Japan based on aircraft monitoring over Sagami Bay, Japan, *J Geophys Res: Atmos*, 110, 2005.

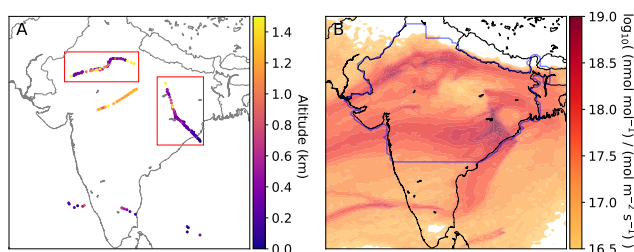


**Figure 1.** (A) Location and altitude of aircraft samples collected over India. The flight paths outlined in boxes were repeated three times each over the sampling period. (B) Average sensitivity to surface emissions from all samples collected over India. A region broadly corresponding to maximum sensitivity in the samples is shown in the blue outline. We denote this region as northern-central India (NCI).

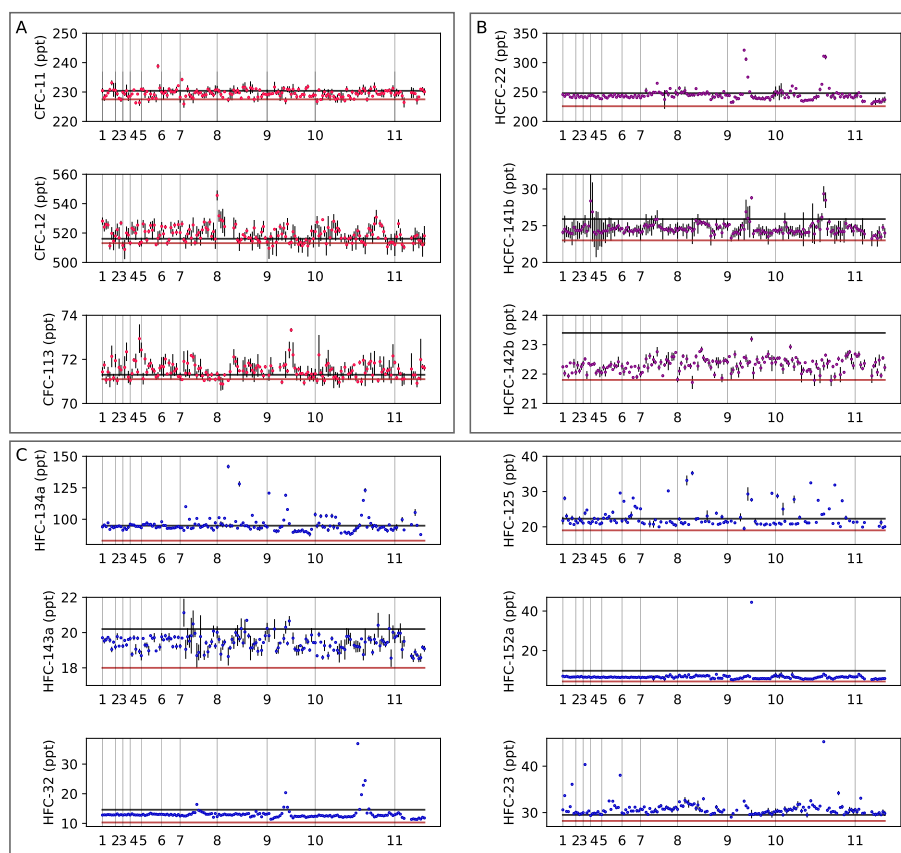


**Figure 2.** (A) CFC, (B) HCFC and (C) HFC mole fraction data from 176 flask samples collected over India, plotted on a flight by flight basis (a summary of flights 1-11 is given in Table 2). Error bars represent instrumental precision, which was estimated using the standard deviation of the three replicate analyses of each flask. Two statistical baselines, inferred from observations at Mace Head, Ireland (black line) in the Northern Hemisphere and Cape Grim, Tasmania (red line) in the Southern Hemisphere, are shown for comparison.

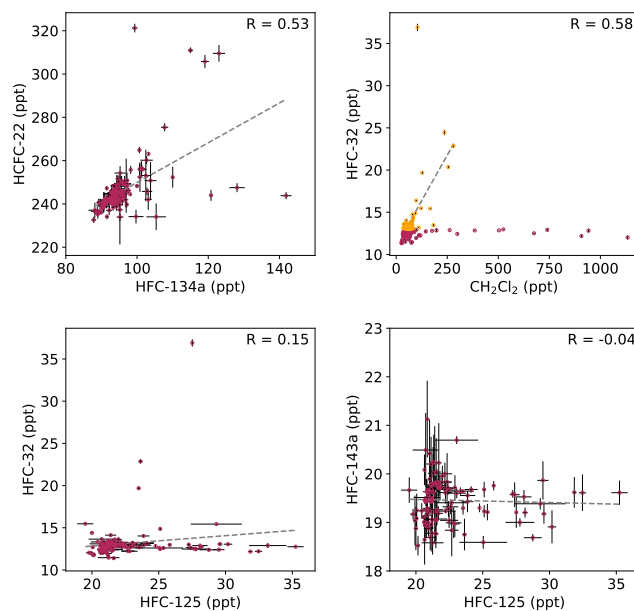


**Figure 3.** Key ODS and HFC scatter plots, shown with line of best fit and respective Pearson correlation coefficient. For HFC-32 vs dichloromethane, the sub-scatter shown in orange is a subset of the dataset corresponding to samples whose HFC-32 mole fraction (lower bound of measurement uncertainty) exceeded the 20<sup>th</sup> percentile of all measurements (and were hence classified as enhanced) since there are other anthropogenic and natural sources of dichloromethane.

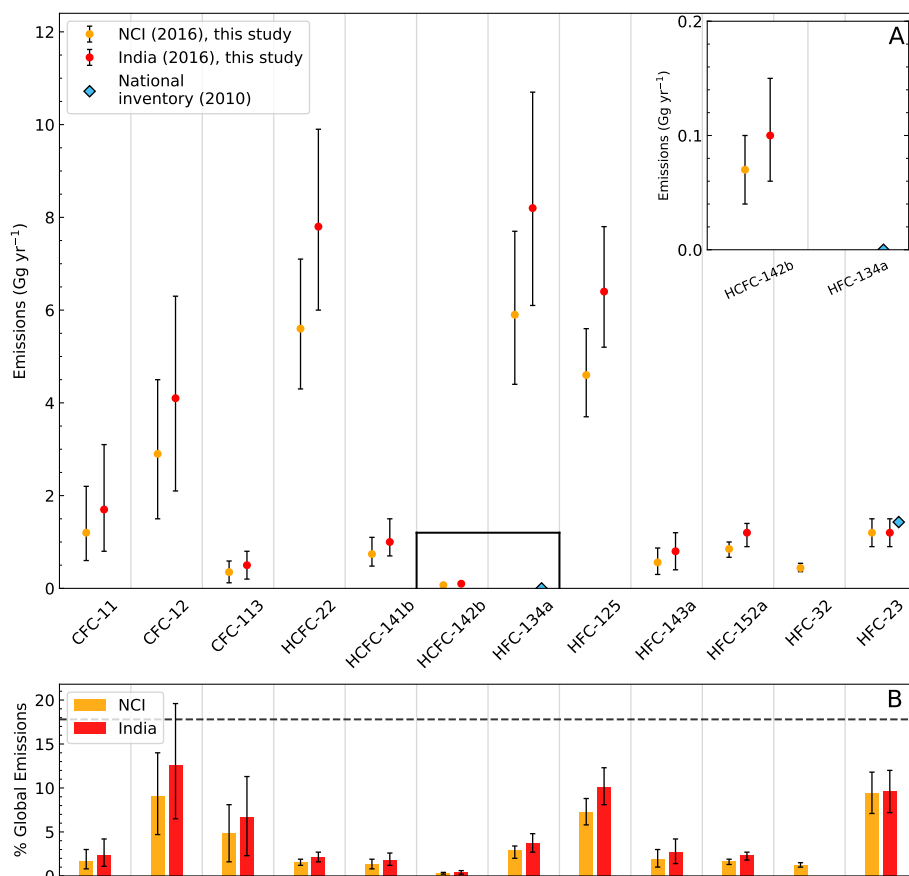


**Figure 4.** (A) NCI (orange) and India total (red) ODS/HFC emissions (Gg yr<sup>-1</sup>) derived in this study. India's most recent greenhouse gas inventory estimates (2010) are included where available. (B) The estimated contribution of the NCI and India to global ODS/HFC emissions (global estimates are an extension of the work by Rigby et al. (2014)). The dashed line represents India's percentage of the global population in 2016. Error bars represent the 5<sup>th</sup>-95<sup>th</sup> percentiles of the posterior distribution.

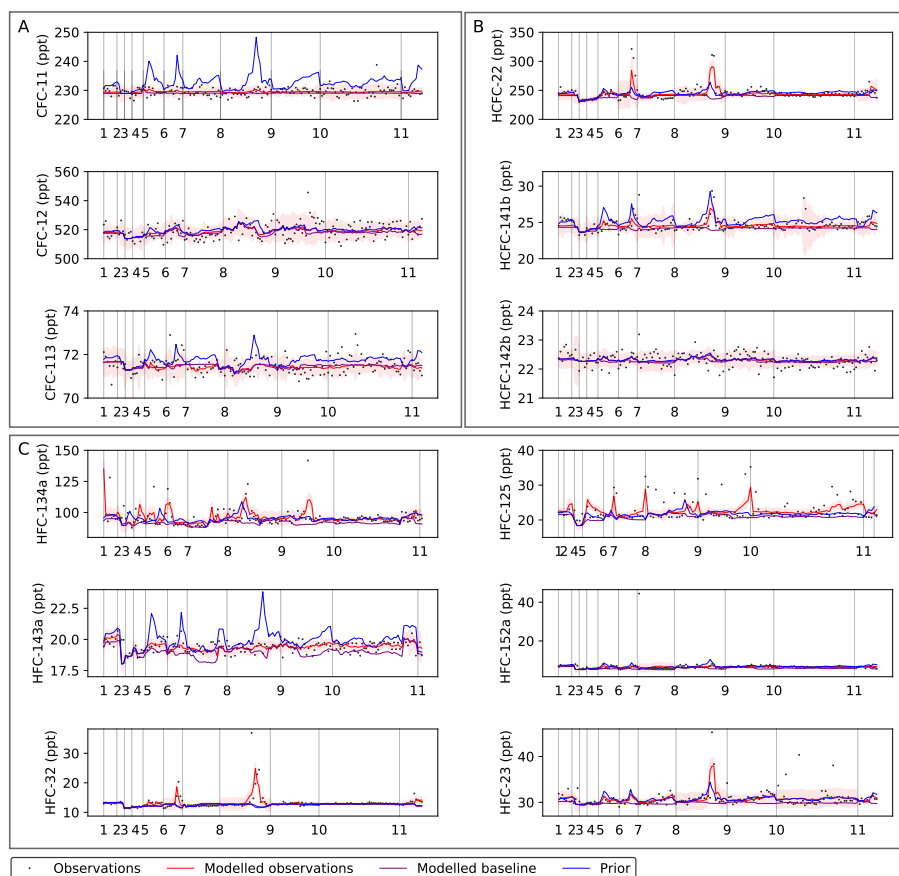


**Figure 5.** Comparison of measured (black points) with prior (blue) and posterior (red line) ODS/HFC mole fraction data, plotted on a flight by flight basis (a summary of flights 1-11 is given in Table 2). The shading represents the model uncertainty ( $5^{th}$  –  $95^{th}$  percentile of the posterior PDF). For all gases, prior emissions were distributed according to the NOAA night light distribution.

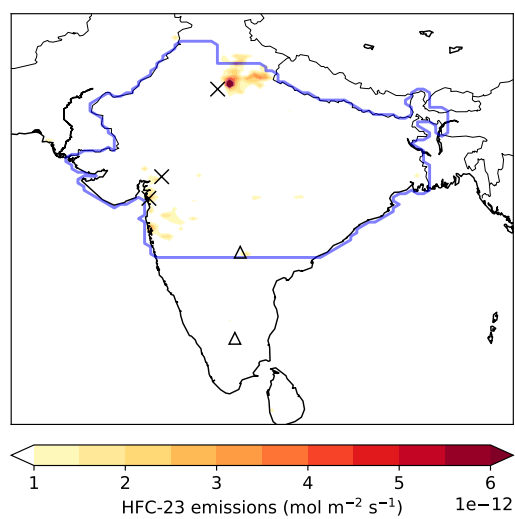


**Figure 6.** Posterior emissions map for HFC-23, reported in  $\text{mol m}^{-2} \text{s}^{-1}$ . The known locations of major ( $> 8 \text{ Gg yr}^{-1}$ ) and minor ( $< 1.5 \text{ Gg yr}^{-1}$ ) manufacturers of HCFC-22 are represented by the crosses and open triangles respectively. The NCI model domain boundaries are given by the blue line.



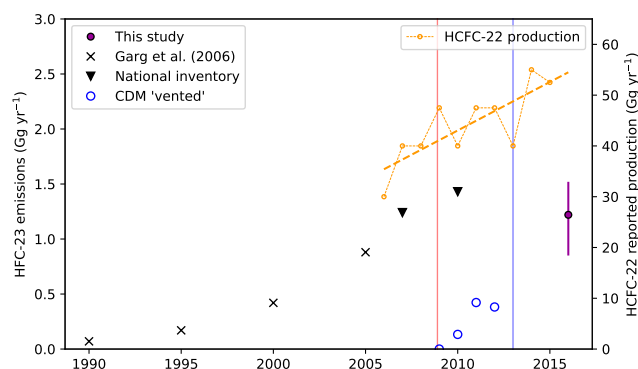


**Figure 7.** HFC-23 emissions ( $\text{Gg yr}^{-1}$ ) from bottom-up and top-down estimates. Bottom-up estimates are from Garg et al. (2006) (black crosses) and India's Second National Communication MoEFCC (2012) and Biennial Update Report MoEFCC (2015) to the UNFCCC for 2007 and 2010, respectively (black triangles). The top-down estimate derived here is plotted as a purple circle with corresponding 5<sup>th</sup>-95<sup>th</sup> percentile uncertainties. Blue circles show the total amount of 'vented' (i.e. released to the atmosphere) HFC-23 per year, as reported by the five HCFC-22 manufacturers during the CDM period. Reported HCFC-22 production ( $\text{Gg yr}^{-1}$ ) data is shown in orange circles and extrapolated to 2016 using a linear fit (dashed orange line). The red bar indicates the first year (2009) in which all five manufacturers of HCFC-22 reported the use of an abatement system and the blue bar indicates the point (January 2013) at which the European Union banned the use of HFC-23 credits under the EU Emissions Trading Scheme. Note the split y-axes – HFC-23 emissions estimates are plotted with respect to the left-hand axis, while HCFC-22 production data is plotted with respect to the right-hand axis.



**Table 1.** Ozone-depleting and greenhouse gases considered in this study. Estimates of lifetime and 100 year global warming potential ( $GWP_{100}$ ) are from Myhre et al. (2013). Ozone depletion potentials (ODP) are from the WMO 2014 Scientific Assessment on Ozone Depletion (Organisation, 2014).

Species	Formula	Lifetime	ODP	$GWP_{100}$	Main application
CFC-11	$CCl_3F$	45.0	1.00	4660	Refrigerant
CFC-12	$CCl_2F_2$	100.0	0.73	10200	Refrigerant
CFC-113	$CCl_2FCClF_2$	85.0	0.81	5820	Solvent
HCFC-22	$CHClF_2$	11.9	0.034	1760	Refrigerant
HCFC-141b	$CH_3CCl_2F$	9.2	0.102	782	Foam-blowing
HCFC-142b	$CH_3CClF_2$	17.2	0.057	1980	Foam-blowing
HFC-134a	$CH_2FCF_3$	13.4	0	1300	Refrigerant
HFC-143a	$CH_3CF_3$	47.1	0	4800	Refrigerant
HFC-125	$CHF_2CF_3$	28.2	0	3170	Refrigerant
HFC-152a	$CH_3CHF_2$	1.5	0	138	Aerosol propellant
HFC-32	$CH_2F_2$	5.2	0	677	Refrigerant
HFC-23	$CHF_3$	222.0	0	12400	By-product

**Table 2.** Aircraft campaign flight summary statistics. All samples were collected during June and July of 2016. IST – Indian Standard Time

Flight number (Fig. 2 label)	Date (time, IST)	Sampling region	Mean altitude (range, km)	Number of samples
B957 (1)	12/06 (06:02 – 07:55)	NE India	1.20 (0.30 – 7.40)	9
B959 (2)	21/06 (08:10 – 08:21)	S India	0.46 (0.05 – 0.87)	2
B963 (3)	25/06 (16:52 – 18:00)	S India	0.31 (0.21 – 0.53)	4
B966 (4)	27/06 (07:12 – 09:49)	S India	0.30 (0.02 – 0.66)	9
B968 (5)	30/06 (05:03 – 06:51)	NW India	0.98 (0.28 – 3.15)	11
B969 (6)	02/07 (05:21 – 07:11)	NW India	0.53 (0.28 – 0.64)	11
B971 (7)	04/07 (07:23 – 08:57)	NE India	0.38 (0.02 – 1.65)	20
B972 (8)	05/07 (05:23 – 07:06)	NW India	0.83 (0.30 – 1.65)	27
B974 (9)	07/07 (06:22 – 07:30)	NW India	1.29 (0.88 – 2.90)	26
B975 (10)	09/07 (06:31 – 08:14)	NE India	0.37 (0.02 – 1.16)	44
B976 (11)	10/07 (06:37 – 07:32)	NW India	0.42 (0.35 – 0.53)	12



**Table 3.** ODS and HFC mass spectrometry target/qualifier ions and respective calibration scales from the Scripps Institution of Oceanography (SIO). Average flask measurement precisions are also shown.

Species	Target ion	Qualifier ion	Calibration scale	Average measurement precision (%)
CFC-11	$\text{CFCl}_2^+$ ( $m/z$ 103)	$\text{CFCl}_2^+$ ( $m/z$ 105)	SIO-05	0.4
CFC-12	$\text{CF}_2\text{Cl}^+$ ( $m/z$ 85)	$\text{CF}_2\text{Cl}^+$ ( $m/z$ 87)	SIO-05	0.7
CFC-113	$\text{CF}_2\text{ClCFCl}^+$ ( $m/z$ 153)	$\text{CF}_2\text{ClCFCl}^+$ ( $m/z$ 155)	SIO-05	0.4
HCFC-22	$\text{CHClF}^+$ ( $m/z$ 67)	$\text{CHF}_2^+$ ( $m/z$ 51)	SIO-05	0.9
HCFC-141b	$\text{CH}_3\text{CFCl}^+$ ( $m/z$ 81)	$\text{CH}_2\text{CCl}_2^+$ ( $m/z$ 61)	SIO-05	3.4
HCFC-142b	$\text{CH}_3\text{CF}_2^+$ ( $m/z$ 65)	$\text{CF}_2\text{Cl}^+$ ( $m/z$ 85)	SIO-05	0.5
HFC-134a	$\text{CH}_2\text{FCF}_2^+$ ( $m/z$ 83)	$\text{CH}_2\text{F}^+$ ( $m/z$ 33)	SIO-05	0.8
HFC-143a	$\text{CH}_3\text{CF}_2^+$ ( $m/z$ 65)	$\text{CH}_2\text{CF}_2^+$ ( $m/z$ 64)	SIO-07	1.3
HFC-125	$\text{CHF}_2\text{CF}_2^+$ ( $m/z$ 101)	$\text{CHF}_2^+$ ( $m/z$ 51)	SIO-15	1.5
HFC-152a	$\text{CH}_3\text{CF}_2^+$ ( $m/z$ 65)	$\text{CH}_2\text{CF}_2^+$ ( $m/z$ 46)	SIO-05	3.2
HFC-32	$\text{CH}_2\text{F}^+$ ( $m/z$ 23)	$\text{CHF}_2^+$ ( $m/z$ 51)	SIO-07	1.1
HFC-23	$\text{CF}_3^+$ ( $m/z$ 69)	$\text{CHF}_2^+$ ( $m/z$ 51)	SIO-07	0.8



**Table 4.** Posterior mean ODS and HFC emission estimates reported in  $\text{Gg yr}^{-1}$  for northern-central India and the whole of India, and the percentage contribution of India to global emissions, where appropriate. The 5<sup>th</sup> and 95<sup>th</sup> percentile ranges are shown in parentheses. HFC-32 is not scaled to an India total since NCI emissions are not considered to be related to population density.

Species	NCI Prior	NCI Posterior	India	% of India to global
CFC-11	9.0 (4.5 – 15.7)	1.2 (0.6 – 2.2)	1.7 (0.8 – 3.1)	2.3 (1.1 – 4.2)
CFC-12	4.1 (1.9 – 7.5)	2.9 (1.5 – 4.5)	4.1 (2.1 – 6.3)	12.6 (6.5 – 19.6)
CFC-113	0.89 (0.58 – 1.28)	0.35 (0.12 – 0.59)	0.49 (0.17 – 0.82)	6.7 (2.3 – 11.3)
HCFC-22	8.0 (5.0 – 12.2)	5.6 (4.3 – 7.1)	7.8 (6.0 – 9.9)	2.1 (1.6 – 2.7)
HCFC-141b	2.1 (1.3 – 3.2)	0.7 (0.5 – 1.1)	1.0 (0.7 – 1.5)	1.8 (1.2 – 2.6)
HCFC-142b	0.09 (0.04 – 0.17)	0.07 (0.04 – 0.10)	0.10 (0.06 – 0.14)	0.4 (0.2 – 0.6)
HFC-134a	5.9 (3.8 – 8.8)	5.9 (4.4 – 7.7)	8.2 (6.1 – 10.7)	3.7 (2.7 – 4.8)
HFC-143a	1.4 (0.6 – 2.7)	0.56 (0.30 – 0.87)	0.8 (0.4 – 1.2)	2.7 (1.4 – 4.2)
HFC-125	1.5 (0.6 – 2.7)	4.6 (3.7 – 5.6)	6.4 (5.2 – 7.8)	10.1 (8.1 – 12.3)
HFC-152a	1.1 (0.6 – 2.0)	0.9 (0.7 – 1.0)	1.2 (0.9 – 1.4)	2.3 (1.8 – 2.7)
HFC-32	0.11 (0.06 – 0.18)	0.44 (0.36 – 0.54)	-	-
HFC-23	1.1 (0.59 – 1.7)	1.2 (0.9 – 1.5)	1.2 (0.9 – 1.5)	9.6 (7.2 – 12.0)



**Table 5.** Posterior mean ODS and HFC emission estimates reported in Tg CO<sub>2</sub>eq yr<sup>-1</sup> for northern-central India and the whole of India. The 5<sup>th</sup> and 95<sup>th</sup> percentile ranges are shown in parentheses. HFC-32 is not scaled to an India total since NCI emissions are not considered to be related to population density.

Species	NCI Prior	NCI Posterior	India
CFC-11	41.9 (21.0 – 73.2)	5.6 (2.8 – 10.3)	7.8 (3.9 – 14.3)
CFC-12	41.8 (19.4 – 76.5)	29.6 (15.3 – 45.9)	41.3 (21.3 – 64.0)
CFC-113	5.2 (3.4 – 7.4)	2.0 (0.7 – 3.4)	2.8 (1.0 – 4.8)
HCFC-22	14.1 (8.8 – 21.5)	9.9 (7.6 – 12.5)	13.8 (10.6 – 17.4)
HCFC-141b	1.6 (1.0 – 2.5)	0.58 (0.38 – 0.86)	0.8 (0.5 – 1.2)
HCFC-142b	0.18 (0.08 – 0.34)	0.14 (0.08 – 0.20)	0.19 (0.11 – 0.28)
HFC-134a	7.7 (4.9 – 11.4)	7.7 (5.7 – 10.0)	10.7 (8.0 – 14.0)
HFC-143a	6.7 (2.9 – 13.0)	2.7 (1.4 – 4.2)	3.8 (2.0 – 5.8)
HFC-125	4.8 (1.9 – 8.6)	14.6 (11.7 – 17.8)	20.3 (16.4 – 24.8)
HFC-152a	0.15 (0.08 – 0.28)	0.12 (0.09 – 0.14)	0.16 (0.13 – 0.19)
HFC-32	0.07 (0.04 – 0.12)	0.30 (0.24 – 0.37)	-
HFC-23	13.6 (7.3 – 21.1)	14.9 (11.2 – 18.6)	15.1 (11.3 – 18.9)